Materials Transactions, Vol. 43, No. 7 (2002) pp. 1633 to 1637
Special Issue on Materials-Related Issues for Cu Interconnects Uned in Ultra High Speed Large Scaled Integrated Si Devices

Formation of Slit-Like Voids at Trench Corners of Damascene Cu Interconnects *1

Atsuko Sekiguchi *2, Junichi Koike and Kouichi Maruyama

Department of Materials Science, Tohoku University, Sendai 980-8579, Japan

Stress voiding was investigated in damascene Cu lines embedded in Ta/TaN/SiO_2/Si. Microstructure was observed before and after heat treatment at 723 K using a focused ion beam (FIB) technique. The distribution of thermal stress was calculated using a three-dimensional finite element method (FEM). FIB observation revealed that slit-like voids were formed at trench shoulders both before and after heat treatment. FEM calculation indicated that a large shear stress concentration occurred at the voided sites. The coincidence between the FIB observation and the FEM calculation suggests that the slit-like voids were formed by shear-mode delamination of Cu from the Ta/TaN barrier layer.

(Received January 21, 2002; Accepted April 4, 2002)

Keywords: *copper, interconnect, void, stress, interface*

1. Introduction

Cu has attracted much attention as a new interconnect material in the place of conventional Al alloys because of its low electric resistance. Combination of the reduction of gate length with the use of Cu interconnect is expected to dramatically increase computing speed as well as cell density. However, poor reliability hampers the full-scale application of Cu to practical devices. One of the major reliability issues during processing is stressmigration that accompanies void formation in Cu and leads to device failure.

Two types of stresses arise during processing. They are growth stress that is present in as-deposited films and thermal stress that arises during heating and cooling cycles. Since the blanket films are under equi-biaxial strain, stress in elastically isotropic crystal becomes equi-biaxial in the entire film volume except near film/substrate interface and surface.[1–5] Such a homogeneous distribution of thermal stress would not cause stress-induced voiding. However, void formation has been reported in blanket Cu thin films after heat treatment.[6–10] Since Cu is elastically anisotropic, shear stress concentration was found to occur along twin interfaces and at twin corners because of the elastic anisotropy of Cu. This stress concentration was considered to act as a driving force for stress-induced voiding.[11] We also found that the voiding tendency was dependent upon twin types. Voids were formed at the interfaces of incoherent {322} twins but not at the interfaces of coherent {111} twins.[12] In the case of damascene Cu lines, it would be interesting to investigate the relationship between voiding and the presence of twins.

Furthermore, the effects of additional stresses caused by surrounding dielectric layers should be taken into consideration. As for stress distribution and void formation in interconnects, Shen *et al*.[13,14] reported theoretical works on stress distribution in Al interconnects and its relation to void formation. They assumed that Al/passivation interface is partly debonded and considered the debonded region as a pre-existing crack. Then, they calculated thermal stress distribution caused by the presence of the pre-existing crack at the interface. They suggested that a particular shear stress distribution would activate dislocation glide with which atoms were carried away from the interface for the crack to grow into a void. However it seems unlikely that all voids are associated with pre-existing crack at interfaces. Moreover, his calculation was performed in two dimenstion with a flat Al interconnect line sandwitched by top and bottom passivation layers. Thus the calculated stress distribution does not represent the stress distribution in damascene Cu lines.

Experimentally, MacDowell *et al*.[15] has reported the distribution of growth strain in Cu damascene lines using a highly focused X-ray diffraction technique with a spacial resolution of a sub-micron range. Although strain variation from one grain to another could be detected, the distribution of strain, or stress, in a much localized scale could not be determined. Because of the limitation in spacial resolution, they made no report on the correlation between stress distribution and void formation. To our knowledge, there has been no published work reporting stress distribution and its relation with stress-induced voiding in damascene Cu lines.

In this paper, we investigated stress distribution and void formation sites in actual damascene Cu lines having various line widths. Stress distribution was calculated using a three dimensional finite element method (FEM). Void formation sites were identified by observing the microstructure before and after heat treatment using a focused ion beam (FIB) machine. Possible correlation was sought to understand a dominant mechanism for stress migration failure in damascene Cu lines.

2. Experimental Procedure

Single crystal (100) Si wafers were used as substrates. Dielectric SiO_2 layer was formed by thermal oxidation to a thickness of 800 nm. Then, using photolithography and plasma dry etching technique, damascene trenches were formed in the SiO_2 layer. Trench depth was set constant at 800 nm, while the width was varied from 150 to 750 nm. The

*1 This Paper was Presented at the Autumn Meeting of the Japan Institute of Metals, held in Fukuoka, on September 23, 2001.
*2 Graduate Student, Tohoku University.

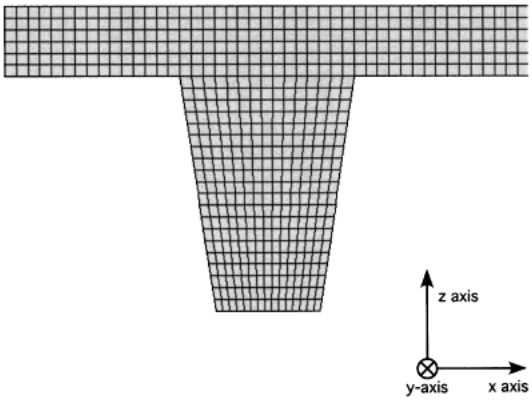

Fig. 1 Schematic drawing of the FEM mesh structure of Cu lines embedded within SiO_2.

line width was defined by the width at the top of the trench. The etching process was followed by PDD sputter deposition of a Ta/TaN diffusion barrier layer and a Cu seed layer. Copper films were electrochemically deposited in the damascene trenches. Deposition was performed to the point where a continuous Cu film, often called an overburden, was formed to approximately 300 nm in thickness over the trench top. These samples were subjected to thermal cycling in a vacuum of 3×10^{-4} Pa at a cooling and heating rate of 3.3 K/min in a temperature range between room temperature and 723 K. Microstructural observation was carried out using a focused ion beam (FIB) apparatus at an accelerating voltage of 30 kV.

3. Calculation of Stress Distribution

Stress distribution in the Cu lines was calculated using a finite-element-method (FEM) computer code, called MARC.[16] Figure 1 shows an example of the FEM mesh structure of Cu lines embedded within SiO_2. Lines were drawn to form the same shape as the experimental damascene lines. Coordinate system was taken to set the X axis along the transverse direction of the line, Y along the longitudinal direction, and Z along the growth direction, *i.e.*, the film normal direction.

In order to examine the thermal stress distribution of Cu lines, we employed the following calculation procedure. Thermal tensile strain was applied to the Cu lines by changing temperature by -100 K from an initial state of zero strain. The calculation was performed only in the Cu lines in an elastic limit without any consideration of plastic deformation. The effects of the surrounding dielectric layer were taken into consideration by fixing the displacement value to zero at the plane contact between Cu and the surrounding layer and by replacing the thermal expansion coefficient of the film by a differential coefficient of $\alpha_{Cu} - \alpha_{SiO_2}$. The effects of the barrier layer were neglected since its thickness was much thinner than those of Cu and SiO_2. In this configuration, the temperature change of -100 K brought about a tensile thermal strain of 1.3×10^{-3}. In our previous work,[11] we reported the importance of the elastic anisotropy effects associated with the microstructure. However, as shown in the result section, void formation in the damascene line was found to be irrelevant to the microstructure probably because of the difference in twin types from the previous reports on blanket films. Therefore, the effects of the microstructure were excluded in the present calculation.

4. Results

Most lines contain no visible defects in as-deposited films of more than 150 nm in width. However, some lines contain void defects. Figure 2 shows some examples of defected lines in as-deposited films, taken by FIB. The line width is 150 nm and 350 nm in (a) and (b), respectively. In both lines, grain size is very small in the order of 100 nm or less. There exist dark contrasted regions, as indicated by arrows, in the middle of the line in (a) and slightly below the shoulder of the trench in (b). The dark-contrasted regions are voids formed during deposition. The voids in the middle of the trench in the 150-nm line are considered to be formed by discontinuous growth of Cu. Since this type of small spherical defects is thermodynamically unstable, no further consideration is given in this paper. On the other hand, in the 350-nm line, the slit-like voids are formed below the trench shoulder remain after heat treatment as shown next. The rest of this paper will focus on the slit-like voids.

Figure 3 shows FIB images of Cu lines after heat treatment. Defects are searched in lines of various widths. Two examples are shown for the lines of 150 and 750 nm in width. In comparison with the as-deposited films in Fig. 2, grain growth by heat treatment is evident. Twin formation is clearly seen as a banded contrast. In the 150-nm line, the left and the right lines contain slit-like voids at the Cu/barrier interface, as indicated by arrows. The contact angle of the void surface with the barrier layer forms an accute angle, indicating that the wettability of Cu on Ta/TaN is poor. Similarly in the 750-nm line, the slit-like voids are observed below the trench shoulder. They are larger in size than the voids in the 150-nm line. It is noted that the shape is not spherical, indicating that diffusion is not a dominant mechanism for the formation of the slit-like voids.

Figure 4 shows calculated stress distribution in 150-nm Cu lines in the X-Z cross section of the FEM coordinate. Tensile stress components are shown in (a)–(c) and shear stress components are shown in (d)–(f). As can be seen in the figure, a large tensile stress of more than 600 MPa arises in the trench interior. The magnitude of tensile stress appears to be the same for all three components. This indicates that the trench interior is under hydrostatic condition. On the other hand, stress value in the overburden is approximately 200 MPa for σ_{11} and σ_{22}, but zero for σ_{33}. This indicates that the stress distribution in the overburden is under a biaxial state, in the same way as continuous blanket films. The difference in stress values and distribution between the trench interior and the overburden results in tensile stress gradient near the trench shoulder. Since the σ_{33} component is zero in the overburden, stress gradient is larger in the Z direction than the other directions. With regard to shear stress distribution, σ_{12} and σ_{23} is approximately zero in the entire trench as well as in the overburden. On the other hand, the σ_{31} component exhibits stress concentration at trench shoulders, acting on the vertical interface in the Z direction. Notice that the stress concentration region extends towards the trench bottom on the vertical interfaces.

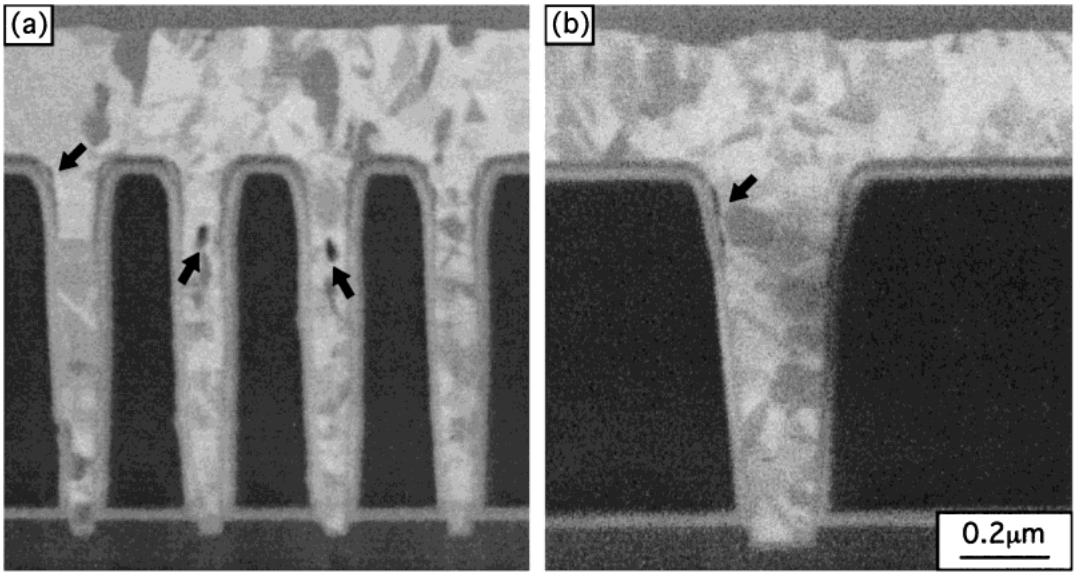

Fig. 2 FIB images of as-deposited damascene Cu lines in width of (a) 150 nm and (b) 350 nm. Voids are formed in the middle of trench and at the trench shoulders indicated by arrows.

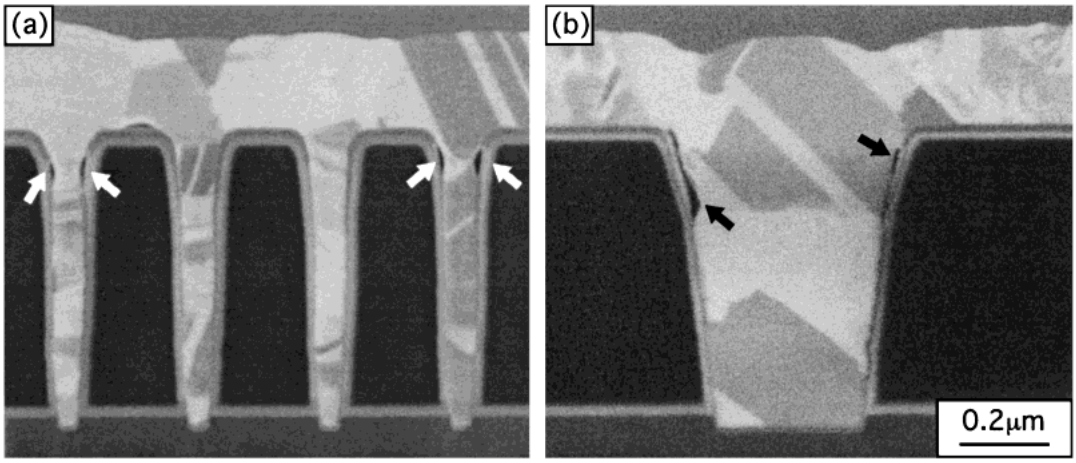

Fig. 3 FIB images of damascene Cu lines after heat treatment. The width is (a) 150 nm and (b) 750 nm. Slit-like voids are formed at the trench shoulders indicated by arrows.

This region coincides with the location of the slit-like voids in Figs. 2 and 3.

The effects of line width on stress distribution can be found by comparing Fig. 4 with Fig. 5. In the same way as in Fig. 4, tensile stresses are shown in (a)–(c), and shear stresses are shown in (d)–(f). In comparison with the 150-nm lines, tensile stress gradient becomes small as indicated by a gradual change in colors. Otherwise, the magnitude of maximum stress in the trench and in the overburden are the same as in the 150-nm lines. The region of shear stress concentration also extends to a wider area on the vertical interfaces. The location and size of the shear concentration region coincide with those of the slit-like voids observed experimentally.

5. Discussion

In the present work, the slit-like voids are observed slightly below the trench shoulder at the Cu/barrier interface both in the as-deposited films and the heat-treated films. Based on the calculated stress distribution, three possible reasons can be considered for the formation of the slit-like voids. The possibilities are (1) stress-induced diffusion under tensile-stress gradient, (2) delamination under tensile stress, and (3) delamination under shear stress. In the following, each possibility is examined.

In blanket Cu films, void formation was found to occur during heat treatment at twin corners and twin intersections.[11] This type of void formation was attributed to tensile stress gradient associated with the elastic anisotropy, *i.e.*, the dependence of elastic moduli on the crystallographic orientations of neighboring grains and twins. Because of the elastic anisotropy effect, void formation sites in the blanket films were closely related to the microstructural features, such as twins and grain boundaries. In the present work, however, no relation can be found between the void formation sites and the microstructural features. This indicates that the microstructural features are not important in void formation in Cu lines.

Even though these microstructural features can be neglected, a substantial gradient of tensile stress is present from the bottom of the trench to the overburden. Since tensile stress takes a minimum value slightly above the trench shoulder, stress-induced diffusion and void formation can take place

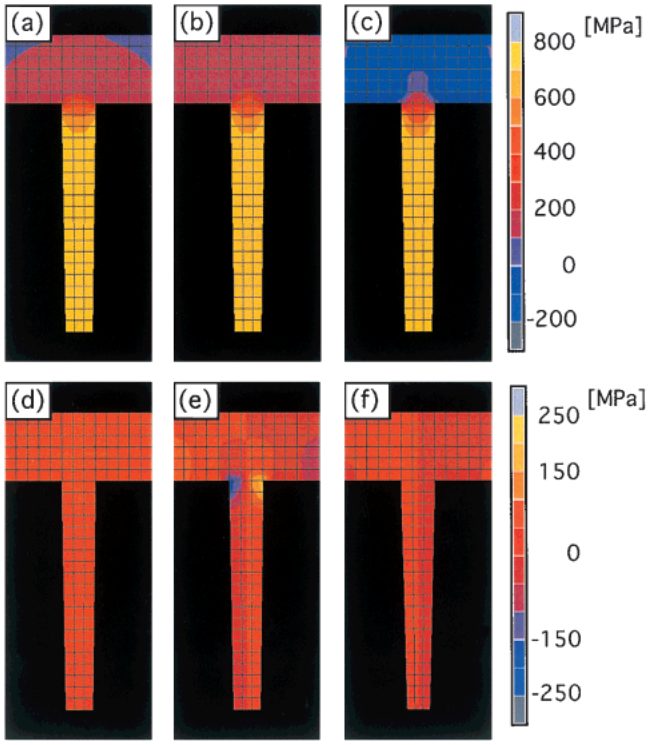

Fig. 4 Calculated stress distribution in 150 nm Cu lines in the X-Z cross section of the FEM coordinate. Tensile stress components are shown in (a)–(c) and shear stress components are shown in (d)–(f). From (a) to (f), the indicated components are σ_{11}, σ_{22}, σ_{33}, σ_{23}, σ_{31} and σ_{12}, respectively.

in this location. However, the slit-like voids are observed slightly below the trench shoulder at the vertical interfaces. Therefore, stress-induced diffusion can be excluded as a possible mechanism. Further support for this statement can be obtained by the fact that the voids are present not only in the heat-treated films but also in the as-deposit films. Therefore, thermally activated process like vacancy diffusion does not play a major role in the formation of the slit-like voids.

As the second possibility of tensile delamination, the calculated stress distribution indicates that a large tensile stress of 660 MPa is distributed in a uniform manner in the lower part of the trench. On the other hand, shear stress concentration gives rise to the maximum value of 160 MPa. Here, it should be noted that no plastic accommodation is allowed for the calculation of stress distribution. If plastic accommodation were to occur, actual tensile stress should be smaller than the calculated value of 660 MPa and would not be in a perfectly hydrostatic state. Bearing this in mind, if tensile delamination occurs, long cracks would be formed along the entire interface in the bottom part of the trench. However, this has never been observed in our samples. The interface in the trench appears to be resistant to tensile delamination.

Finally, the possibility of shear delamination is discussed. As shown in Figs. 3 and 4, a remarkable coincidence is found in the size and location of the slit-like voids with those of shear stress concentration. This coincidence suggests that shear stress concentration is a principal reason for the formation of slit-like voids. Since shear stress does not accompany volume change nor stress-induced diffusion, delamination is proposed as a void formation mechanism. The shear delamination is also consistent with a thermal formation of slit-like voids observed in the as-deposited films. Generally, biaxial stress components in as-deposited Cu films are in a tensile state. The magnitude of the biaxial stress is larger at room temperature than at elevated temperatures. Since the residual stress in the as-deposited films arises because of the confinement of Cu to the substrate, residual stress distribution should be the same as the calculated distribution of thermal stress in the heat-treated films. In this regard, shear stress concentration is expected to occur at the same location in the as-deposited film as in the heat-treated films. Thus, slit-like voids are considered to be formed by a shear delamination mechanism.

In order to prevent the formation of the slit-like voids, interface bond strength should be improved. The interface bond strength has been investigated in detail by Lane and Dauskardt for blanket Cu films.[17,18] They measured critical interface fracture energy in various Cu/barrier/SiO_2/Si samples using a four-point bending method. The barrier layers were Ta and TaN of different N concentrations and a notch was formed in the Si substrate. In their experiments, delamination was observed always at barrier/SiO_2 interfaces. On the other hand, the slit-like voids observed in the present work is formed at the Cu/barrier interface. Although the discrepancy in delamination sites cannot be explained at the moment, delamination is an important issue for interconnect reliability. Further work is necessary to understand the correlation between processing conditions and delamination strength, and to understand physical and chemical factors to control delamination strength.

6. Summary

Void formation was observed by FIB in damascene Cu lines before and after heat treatment at 723 K. Slit-like voids were found at trench shoulders along Cu/barrier interfaces in both as-deposited lines and heat-treated lines. No correlation was found between the void formation sites and the microstructure of the lines, such as twin interfaces and grain boundaries. Three-dimensional FEM analysis indicated that tensile-stress gradient was present from a trench bottom towards an overburden and that a localized shear stress concentration was present at trench shoulders. A good coincidence was found between the shear concentration sites and the voided sites. This coincidence suggests that the origin of the slit-like void formation is shear-mode delamination under shear stress concentration.

Acknowledgements

One of the authors (A.S.) is grateful for a financial support by Sasakawa Scientific Research Grant from The Japan Science Society. This work was partly supported by Grant-in-Aid for Scientific Research, Ministry of Sports, Science, Education and Culture of Japan (#13450281), and by NEDO Nanotechnolgy Program on Cu Thin Films. We also thank Dr. G. Chung, Mr. Sato, and Mr. Marumo of Tokyo Electron Ltd. for providing the samples.

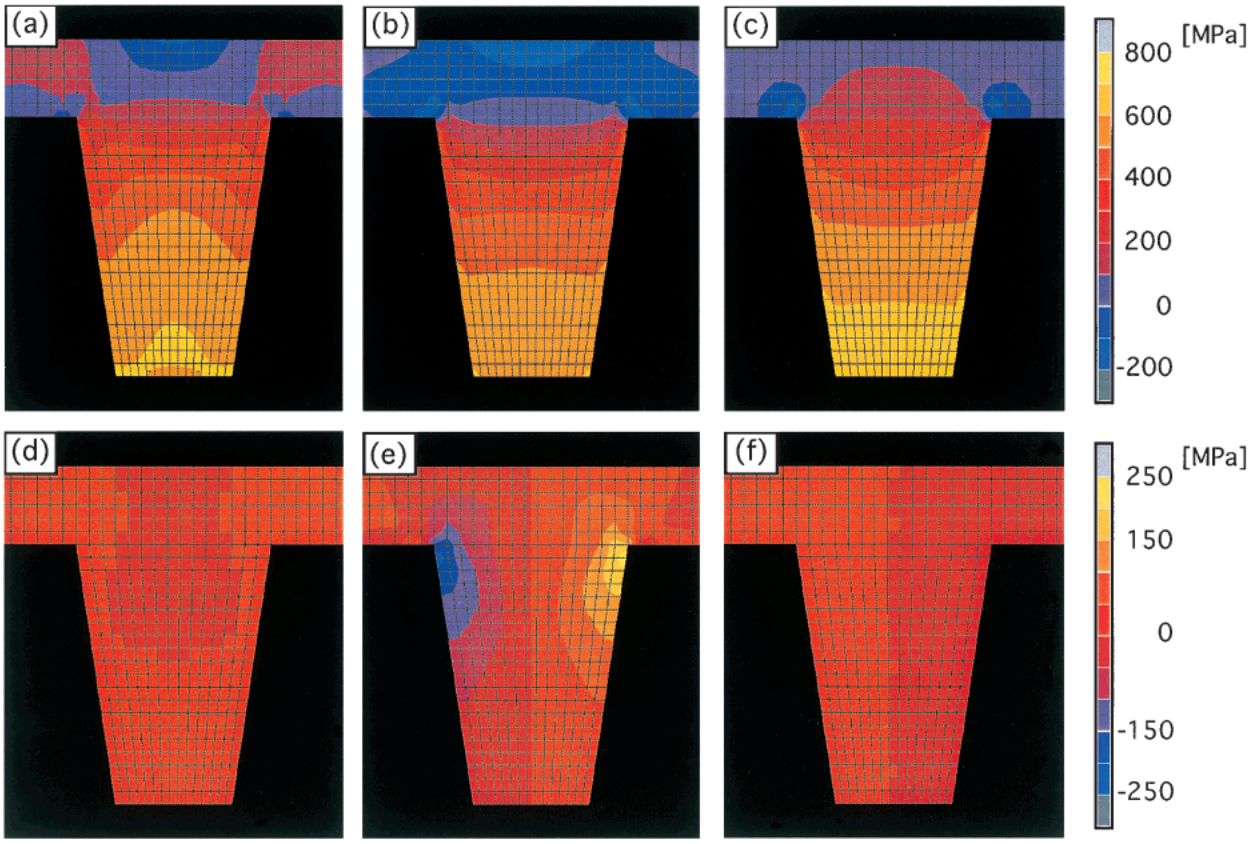

Fig. 5 Calculated stress distribution in 750 nm Cu lines in the X-Z cross section of the FEM coordinate. Tensile stress components are shown in (a)–(c) and shear stress components are shown in (d)–(f). The indicated stress components are the same as in Fig. 4.

REFERENCES

1) M. D. Thouless, J. Gupta and J. M. E. Harpar: J. Mater. Res. **8** (1993) 1845–1852.
2) R. P. Vinci, E. M. Zielinski and J. C. Bravman: Thin Solid Films. **262** (1995) 142–153.
3) R. M. Keller, S. P. Baker and E. Arzt: J. Mater. Res. **13** (1998) 1307–1317.
4) R. M. Keller, S. P. Baker and E. Arzt: Acta. Mater. **47** (1999) 415–426.
5) M. J. Kobrinsky, C. V. Thompson and M. E. Gross: J. Appl. Phys. **89** (2001) 91–98.
6) P. Borgesen, J. K. Lee, R. Gleixner and C. Y. Li: Appl. Phys. Lett. **60** (1992) 1706–1708.
7) J. A. Nucci, Y. Shacham-Diamond and J. E. Sanchez, Jr.: Appl. Phys. Lett. **66** (1995) 3585–3587.
8) J. A. Nucci, R. R. Keller, J. E. Sanchez, Jr and Y. Shacham-Diamond: Appl. Phys. Lett. **69** (1996) 4017–4019.
9) R. R. Keller, J. A. Nucci and D. P. Field: J. Electron. Mater. **26** (1997) 996–1001.
10) J. A. Nucci, R. R. Keller, D. P. Field and Y. Shacham-Diamond: Appl. Phys. Lett. **70** (1997) 1242–1244.
11) A. Sekiguchi, J. Koike, S. Kamiya, M. Saka and K. Maruyama: Appl. Phys. Lett. **79** (2001) 1264–1266.
12) J. Koike, A. Sekiguchi, M. Wada and K. Maruyama: AIP conf. Proc. (2002) in press.
13) Y. L. Shen: J.Mater.Res. **14** (1999) 584–591.
14) Y. L. Shen, Y. L. Guo and C. A. Minor: Acta. Mater. **48** (2000) 1667–1678.
15) A. A. MacDowell, R. S. Celestre, N. Tamura, R. Spolenak, B. Valek, W. L. Brown, J. C. Bravman, H. A. Padmore, B. W. Batterman and J. R. Patel: Nucl. Instrum. Methods. **467–468** (2001) 936–943.
16) Copyright reserved by MSC Software Corporation.
17) M. Lane, N. Krishna, I. Hashim and R. H. Dauskardt: J. Mater. Res. **15** (2000) 203–211.
18) M. Lane, A. Vainchtein, H. Gao and R. H. Dauskardt: J. Mater. Res. **15** (2000) 2758–2769.